

EFFECTIVE CBIR BASED ON HYBRID IMAGE FEATURES AND MULTILEVEL APPROACH

V. ARCHANA REDDY, V. VIJAYA KUMAR

¹Research Scholar, school of engineering, Anurag University, Hyderabad, India

²Professor, school of engineering, Anurag University, Hyderabad, India

Corresponding author Email: vareddy.cse@gmail.com , drvvk144@gmail.com

ABSTRACT

The instantaneous search and retrieval of the most relevant images to a specific query is one of the significant applications of image processing. The process of retrieval of images using image contents is widely known as content base image retrieval (CBIR). The image features extracted from the local windows of 3×3 resulted good results in CBIR. However, the micro windows of 2×2 derived the texton and motif features and played a dominant role in CBIR. This paper segmented the 3×3 window into two windows namely cross and diagonal windows. Four directional motifs of 1×3 are extracted from each of the cross and diagonal segments. The motif features are derived using Rule based Directional motif (RDM) to address the ambiguity issues. This paper transformed the motif indexes derived on a 1×3 triangular window to a 3×3 window and derived eight triangular RDM local units. The local features are extracted by integrating the features extracted from the eight different images. The extracted features hold directional, textures, patterns, edge properties derived from the 3×3 and triangular windows. The results indicate the superiority of the proposed methods.

Key words: 3×3 Window, 1×3 Triangular Window, Directional Motif;

1. INTRODUCTION

Internet applications are introducing tremendously large amounts of images into databases of server and even retrieval of images of large quantities is brought about through databases. The phenomenon portrays the CBIR system as very essential. The initial steps of image retrieval algorithm are related to text-based query on the basis of text annotation model [11], Jing [24] that clients require a significant amount of man-power to tag every image on the database. Human perception will create some misjudgment in annotation and to overcome such a problem the system based on content technology to be formed where, they will be taken to retrieve image-wise. Therefore, a better retrieval mechanism was introduced as content-base image retrieval (CBIR) system in the 80s. Based on this process the pictures are retrieved with the help of the database that allows to the picture content. The main task of this CBIR system is the creation of image feature sets in terms of color, texture and shape of the images.

Bian et al. [2] introduce a CBIR method. The important point on this aspect is the multichannel decoded local binary patterns. The benefit lies in the generic application of

the natural and the textural images. The cost of this is the increase in retrieval time since the high dimension of the decoder-based descriptor consumes a lot of time. The authors Husain and Bober [5] propose a special scheme of building image retrieval. The author has work on the rank assignment of multiple clusters based on the use of local descriptors. Cluster normalization is conducted in each cluster according to the direction network conservation, and the aggregation of neighborhood rank. The strategy leads to a post-PCA normalization strategy to achieve an effective choice campaign between matching and no matching descriptors. The lengthy running procedure is induced by the complicated structure of the routine. In Yang et al. [9] a quick and intuitive approach to image retrieval is offered. The method starts with extract features based on Color Co-occurrence Matrix (CCM), Difference between pixels of scan pattern (DBPSP), Local Binary Pattern (LBP) and Histogram of oriented gradients (HoG). These are followed by transformation of feature dimensionality. Lastly, a new distance theory is included to choose the most pertinent image in the retrieval samples. Nevertheless, the drawback

of this approach is that additional features could also be extracted in order to enhance retrieval rates. Subash Kumar and Nagarajan [8] describe a new LBP based CBIR approach on natural images. To tune the performance, the image pixels through which the pattern is extracted are chosen in run time in consideration of the characters of the image. This method is based on the identification of the local pattern with the image line/curve properties which are referred to as Local Curve Pattern (LCP). The drawback of this method is it does not involve deep learning to enhance the performance. The good aspect about the run time selection of pattern.

Srivastava and Khare [7] describe a CBIR system based on multiscale LBP, where the LBP is calculated on different groupings of the neighborhood pixels (eight) in the vicinity of a center pixel at a number of scales. The ultimate characterizing rose-garden is produced by the Gray Level Co-occurrence Matrix (GLCM). The major advantage of the multiscale LBP method over the single-scale LBP is that it overcomes the drawbacks of the single-scale one. The approach, however, does not assume image moments, so it is a setback [15]. Agarwal et al. [1] propose a feature, the multi-channel local ternary pattern. The approach abstracts cross channel color-textural color by integrating the three H-V, S-V and V-V channels of the HSV feature space of the picture. Due to the simultaneous acquisition of color and texture data, the method leads to a detailed image description, which is the methodological drawback of the method. In spite of this, it becomes useful in the contemporary applications as it excels in image retrieval tasks.

Although so many methods were projected, each method had downsides and incompetence primarily in terms of retrieval accuracy and execution time. These drawbacks are mainly prone by the less capable image descriptors incorporated in the existing methods. So, a new CBIR methodology is proposed in this paper to minimize the drawbacks of the existing method. A large number of repositories have emerged in areas as diverse as architecture, astronomy, education, geology, medicine, multimedia and remote sensing, among others. There is even greater necessity of efficient storage and access and thus the CBIR systems cannot be ignored as the volume of available images is rising substantially. Such systems are

applied a lot in the real world, e.g. to crime prevention, digital libraries, medical diagnostics, textile industry, and traffic congestion analysis. The problem that comes to the fore in CBIR is the selection of such features that are effective in reducing how similar two images are to each other, but also consume little space. Also, the construct of similarity available to the human eye is both subjective and semantic and hence task-oriented, difficult to measure by the classical filter-based features like color, shape or texture. This is the so-called semantic gap: the lack of alignment between rich concepts encoded by an image (e.g. emotions, events or objects) with the limited descriptive capabilities of low censored visual features [2, 15, 16].

This paper is organized as follows: the section 2 and 3 presents methodology with a precise algorithm and database description. The section 4 and 5 gives the results and discussions and conclusions.

2. METHODOLOGY

Motifs are defined on a 2x2 grid. Basically, the motif defines the structural behavior of the grid. In the basic motif on the 2*2 grid [31] the peano scan position always starts from the left most corner pixel of the 2x2 grid, irrespective of its grey level behavior with the other pixels on the grid (fig 1). This restricts it from generating wide spread of structuring elements. This generates only six motifs as given in fig 1:

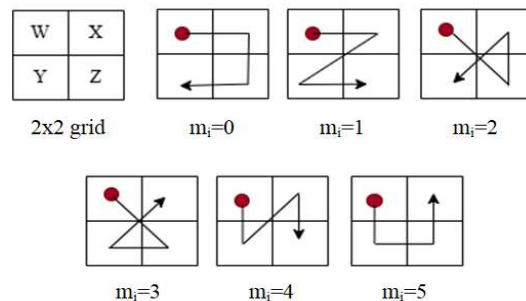


Figure 1: Six Peano motifs on a 2x2 grid

In the dynamic motif [32] the scan position is **initiated** from the pixel position whose gray level value is the least (fig 2). The dynamic motif (DM) generates a good number of different structural patterns or motifs as given in fig 2. This enhances the discrimination power.

Consequently, DM picks up 24 unique motif indices (0 to 23) that represent diverse structural arrangement within the 2x2 grid. The DM, increased the motif indexes from six to twenty-four, however this could not yield good retrieval rate. This is due to the ambiguity created in choosing the initial or next scan position, whenever two or more Pixels exhibits the same attributes i.e grey levels (this is also same for the basic motif of fig. 1).

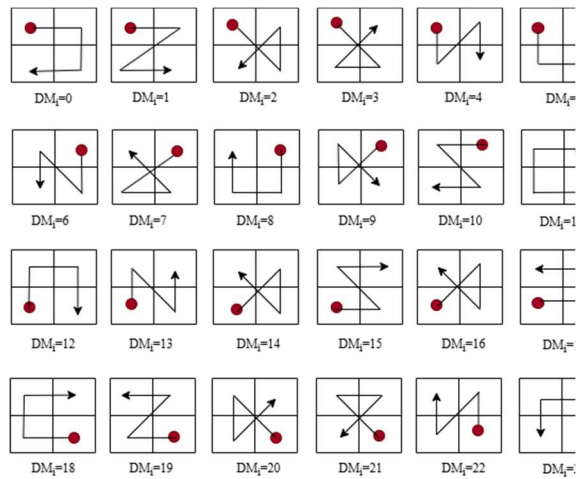


Figure 2. 24-Different Motif By A Dynamic Motif Grid

This is addressed by rule based Motif [31,32]. On a 2*2 grid, whenever two or more pixels exhibits the similar intensities, the ambiguities in the next scan position can be overcome by giving preference to left column over right column and top row over bottom row. It is explained for dynamic motifs with the figure 3 .

1. The way the ambiguities are overcome in DM by rule-based motif is shown fig.3, 4 and 5. The fig 3 and 4 displays the ambiguities in assigning a unique motif with three and two identical pixels of analogous attributes respectively.

2. The way the rule-based motif has overcome the ambiguities is explained in fig 5.

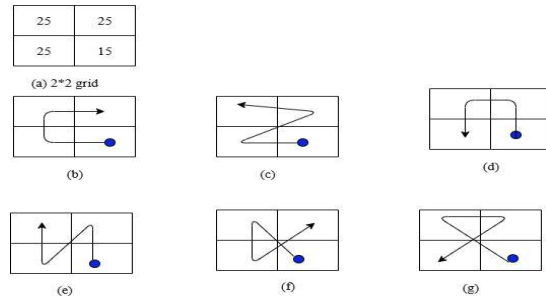


Fig 3: Ambiguity Issues In Scan Positions With Three Identical Pixels

The figure 3(a) represents a 2*2 grid with exactly similar behavior from three pixels. The dynamic motif results six different scan directions or 6 possibilities of different motif index and they are show in 3.b to 3.g. The DM fails in generating a unique motif index and further creates an ambiguity.

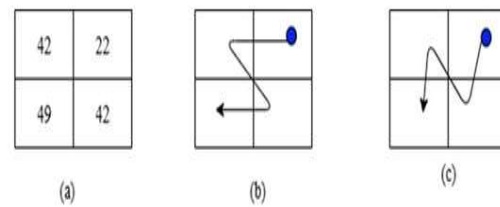
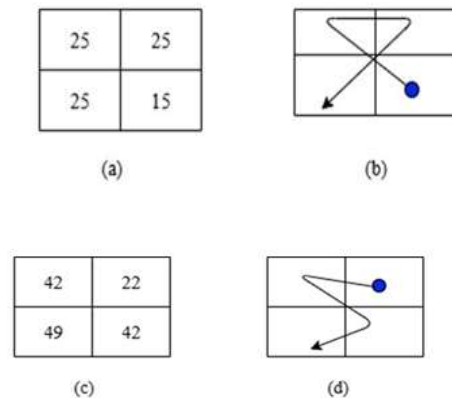


Fig 4: Ambiguity Issues: 2-Pixels With Similar Grey Levels

In the similar way, whenever the two pixels shows the same behavioral aspects then it results two different motif indexes in the case of dynamic motif and it leads to ambiguity as shown in the fig 4.



(a). 2*2 grid with 3-identical pixel; (b). The unique representation by DM of fig (a) ; (c): grid

with 2 similar grey levels; (d): a unique representation of fig. c by DM;

Fig 5: A Unique Representation By Rule-Based Motif

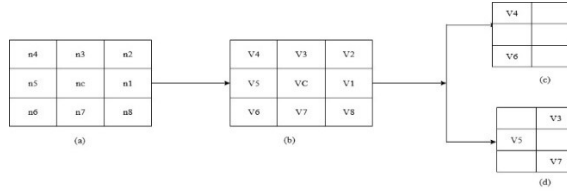


Fig 6: The Derivation Of Cross Matrix (CM) And Diagonal Matrix (DM)

$$V_i = \text{abs}(n_c - n_i) \quad (1)$$

where $i = 1$ to 8

The present research divides the input image into a 3×3 window in an overlapped manner. The 3×3 window is represented with eight neighboring pixels n_1 to n_8 and center pixel n_c as shown in the figure 6(a).

On the 3×3 grid absolute differences are computed as per equation 1. The neighboring pixels after absolute differences are denoted as $V_1 \dots V_8$. This 3×3 grid is divided into cross and diagonal matrices (CDM), of four neighboring pixels each, as shown in the fig 6.d and 6.c respectively. The V_2, V_4, V_6 and V_8 constitutes the diagonal matrix (DM) and in the similar way the V_1, V_3, V_5 and V_7 represents the of cross matrix (CM) of the 3×3 window. (fig. 6.c and 6.d).

This paper derived four 1×3 smart Triangular Directional Motif (TDM) grids based on a directional information from each of CM and DM. The direction motifs derived on Cross and diagonal matrix are named as Cross-TDM (CTDM) and Diagonal-TDM (DTDM) respectively. Each of CTDM and DTDM derives for different TDM's, with 3 pixels each. The four DTDM's are denoted as DTDM1 to DTDM4 (fig 7) and the four CTDMs are denoted as CTDM1 to CTDM4 (fig 8). Each of CTDM1 to CTDM4 and DTDM1 to DTDM4 are different with respect to angle of rotation measured with respect to center pixel of the 3×3 grid. The Fig.9 displays the directional angle of rotations of neighboring pixels with respect to center pixel on a 3×3 grid.

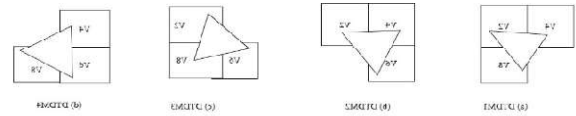


Fig 7: The Derivation Of Four Diagonal TDM (DTDM) of size 1×3 from a given DM (a) DTDM1: $(45^\circ, 135^\circ$ and $315^\circ)$; (b) DTDM2: $(45^\circ, 135^\circ, 225^\circ)$; (c) DTDM3: $(45^\circ, 225^\circ, 315^\circ)$; (d) DTDM4: $(135^\circ, 225^\circ, 315^\circ)$

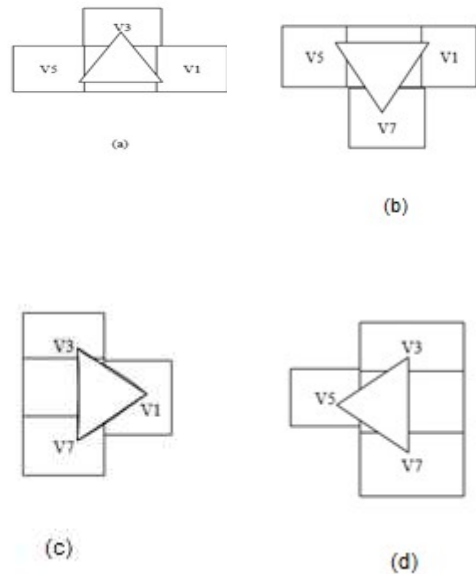


Fig 8: The Derivations Of Four Cross TDM (CTDM) On A 3×3 Window

- (a) CTDM1: $(0^\circ, 90^\circ, 18^\circ)$; (b) CTDM2: $(0^\circ, 180^\circ, 270^\circ)$; (c) CTDM3: $(0^\circ, 90^\circ, 270^\circ)$; (d) CTDM4: $(90^\circ, 180^\circ, 270^\circ)$

135° V4	90° V3	45° V2
180° V5	VC	0° V1
225° V6	270° V7	315° V8

Fig 9: A 3×3 Window With Angle Of Rotation.

The aim is to determine a unique motif index for each of CTDM and DTDM. The possible formation of motif indexes for CTDM1 is displayed below in fig 10.

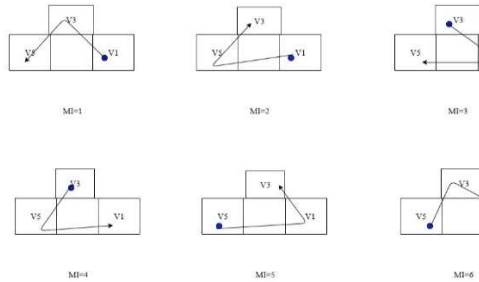


Fig 10 : The Possible Formation Of Peano Scan Directions (PSD) Or Motif Index (MI) For CTDM1 (0°, 90°, 180°)

In the above fig.10, the V1, V3 and V5 represents the triangular grid formed by using three neighboring pixels of cross matrix of the 3x3 window. And they form a directional angle of 0°, 90°, 180° respectively with respect to central pixel. (the rotational angles of neighboring pixels: $V1^\circ < V3^\circ < V5^\circ$). The motifs generate ambiguity or two more PSD if two or more pixels exhibits exactly similar behavior. This ambiguity results, two or more different structural pattern indexes or motif indexes for the same 2x2 grid. This phenomenon reduces drastically overall retrieval rate. This is addressed in this research by deriving a new method “Rule based Directional Motif (RDM)”. If two or more pixels exhibits the similar grey level values, the RDM initiates the next PSD from the pixel position, whose directional angle is the least. This is explained with the following two cases for CTDM1:

Case:1 Let all three pixels of CTDM1 exhibits the same grey levels: $V1 \equiv V3 \equiv V5$ (FIG. 11 (b)) ; in this case the ordinary motif derives 6 different motif indexes. This has been resolved by RDM: since all three pixels exhibits the similar behavior, the scan position starts from the pixel position whose angle of rotation is least with respect to center pixel, in this case it is V1. then followed by V3 and V5. fig.11(b).

Case: 2: the two pixels exhibits the same brightness value: $V1 = V5$ (Fig. 11 (c)). In this case, the scan position starts from V3, since the brightness value is least. Then there is an ambiguity, in the next scan position, since both V1 and V5 holds the same intensities. This is resolved by RDM by giving preference to the pixel position whose angle of direction is least, i.e., V1 (fig.11(c)).

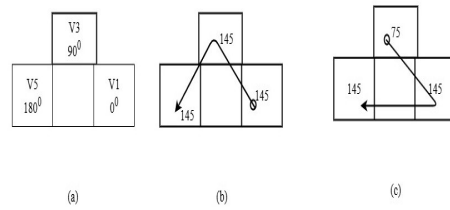


Figure 11: Resolving Ambiguities By RDM

The other advantage of RDM is it reduces the overall scan directions or motif index into ‘6’ categories as shown in fig 10. The RDM index for the CTDM1 will be denoted as CT-RDM₁ and represented mathematically by considering RDM principles of fig.11.

$$M_1 (0^\circ, 90^\circ, 180^\circ) = 1. (V1 \leq V3) \ \&\& \ (V3 \leq V5)$$

$$CT-RDM_1 \quad 2. (V1 \leq V5) \ \&\& \ (V5 < V3)$$

$$3. (V3 < V1) \ \&\& \ (V1 \leq V5)$$

$$4. (V3 \leq V5) \ \&\& \ (V5 < V1)$$

$$5. (V5 < V1) \ \&\& \ (V1 \leq V3)$$

$$6. (V5 < V3) \ \&\& \ (V3 < V1)$$

(2) where V1 , V3 and V5 are the brightness value of the triangular grid of the image further the angle of V1 , V3 and V5 are 0°, 90° and 180° respectively. Further the directional angle of rotations holds the relationship $V1^0 < V3^0 < V5^0$. This Paper aims to transform the input image into CT-RDM1 image based on the pixel behavior in the direction of 0°, 90°, 180°. The detailed explanation of deriving unique motif number or index is given below for few cases: of CT-RDM1:

1. **For motif 1:** Let V1 and V3 and V5 be 40,50 and 60 respectively i.e ($V1 < V3 < V5$), in this case the 1*3 pattern is replaced by an index 1 or let V1, V3 and V5 be 40,40 and 40 respectively. In this case all three pixels exhibits the same intensity value and the conflict or ambiguity in choosing initial position is resolved by RDM i.e, initiates the scan position from V1 since angle of rotation is least i.e 0°. Then V3 and followed by V5. (since angle of rotation of $V3^0 < V5^0$)

2. **For motif 3:** in this case the V3 brightness is least when compared to V1 and V5 . The scan position begins from V3. Even if $V1 = V5$ the next Scan position will be initiated from V1 as directed by RDM.

3. **For motif 6:** The intensity of $V_5 < V_3 < V_1$ the scan position begins from V_5 then V_3 (since $V_3 < V_1$) and finally the scan position ends with V_1

This process is repeated on the entire image in an overlapped manner. This transforms the input image in to a CT-RDM1 image, with index values ranging from 1 to 6. In the same way CT-RDM2, CT-RDM3 and CT-RDM4 indexes are computed and the input image is transformed in to three different images i.e, CT-RDM2, CT-RDM3 and CT-RDM4 images. Thus, the CTDM1, CTDM2, CTDM3 and CTDM4 of fig 8 generates four different images namely CT-RDM1 to CT-RDM4 respectively. On each of the CT-RDM image Local Binary Pattern units (LBPu) is derived by using XOR patterns. The center pixel is replaced by LBPu. The LBPu ranges from 0 to 255. The XOR pattern is derived by computing XOR relationship on each of the neighboring CT-RDM index with respect to center pixel. The computation process of LBPu on the CT-RDM1 image is shown in fig 12. And this process is implemented in an overlapped manner on the entire image. This process transforms the CT-RDM1 image into CT-RDM- Local unit1 (CT-RDMLU1) image.

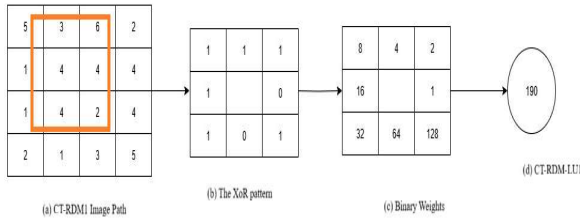


Figure 12: Transformation Of CT-RDM1 Image Into CT-RDMLU1.

$$CT - RDMLU1 = (\sum_{i=0}^7 CT - RDM_1(P_i, P_c) * 2^i) \quad (3)$$

$$CT - RDM1(P_i, P_c) = \begin{cases} 1 & P_i \neq P_c \\ 0 & P_i == P_c \end{cases} \quad (4)$$

Once the CT-RDM1 image is transformed into CT-RDMLU1 image, a histogram is built on the entire image, as given in equation 5.

$$H - CT - RDMLU1 = \sum_{i=0}^{N-1} \sum_{j=0}^{M-1} (F(CT - RDMLU_1(i, j), U)) \quad (5)$$

Where U belongs to [0,255] and N*M is the size of the image.

In the similar manner CTRDM2, CTRDM3, and CTRDM4, images are transformed into CT-RDMLU2, CT-RDMLU3 and CT-RDMU4 images respectively and the respective histograms are computed. Finally, the Feature vector of CT-RDMu is computed by concatenating the four directional histograms as given in equation 6

$$CTRDM_U = [H - CTRDMLU1; H - CTRDMLU2; H - CTRDMLU3; H - CTRDMLU4] \quad (6)$$

The feature vector size of CTRDMU ranges from 0 to 1023.

This paper transforms the DTDM1, DTDM2, DTDM3 and DTDM4 of fig 7 into DT-RDM1, DT-RDM2, DT-RDM3 and DT-RDM4 images respectively. The detailed explanation of deriving unique motif number or index for DT-RDM4: $(135^0, 225^0, 315^0)$ is given mathematically below:

$$M_l(135^0, 225^0, 315^0) = 1. (V_4 \leq V_6) \ \&\& \ (V_6 \leq V_8) \\ DT-RDM4 \quad 2. (V_4 \leq V_8) \ \&\& \ (V_8 < V_6) \\ 3. (V_6 < V_4) \ \&\& \ (V_4 \leq V_8) \\ 4. (V_6 \leq V_8) \ \&\& \ (V_8 < V_4) \\ 5. (V_8 < V_4) \ \&\& \ (V_1 \leq V_6) \\ 6. (V_8 < V_6) \ \&\& \ (V_6 < V_4) \quad (7)$$

where V_4, V_6 and V_8 are the brightness value of the triangular grid. Further the directional angle of rotations holds the relationship $V_4^0 < V_6^0 < V_8^0$.

The derived motif index patterns of 2,4,6 of DTRDM4 are explained below.

1. For motif 2: Let V_4 and V_6 and V_8 be 40,60 and 50 respectively i.e $(V_4 < V_8 < V_6)$, in this case the 1*3 pattern is replaced by an index 2 or let V_4, V_6 and V_8 be 40,60 and 40 respectively. In this case the two pixels V_4 and V_8 exhibits the same intensity value and the conflict or ambiguity in choosing initial position is resolved by RDM i.e, initiates the scan position from V_4 since angle of rotation is least i.e 135° . Then V_8 and followed by V_6 . (since $V_8 < V_6$)

2. For Motif 4: Let V_4, V_6, V_8 be 70,40,50 in this case PSD initiates from v_6 then proceeds V_8 and then V_4 since V_6

$V_8 < V_4$. Let V_4, V_6 and V_8 be 70, 40 and 40. There is an ambiguity in choosing initial PSD this is addressed by RDM by choosing V_6 , since angle of rotation of $V_6 <$ angle of rotation of V_8 .

3. For motif 6: The intensity of $V_8 < V_6 < V_4$ the scan position begins from V_8 then V_6 (since $V_8 < V_6$) and finally the scan position ends with V_4 .

The DT-RDM images are represented by the motif index ranging from 1 to 6. The DT-RDM_i images are transformed into DT-RDMLU_i images by using XOR operation on the 3*3 grid. This histogram of DT-RDMLU₁ to DT-RDMLU₄ are computed and concatenated to derive DT-RDMU. The Feature vector of DT-RDMLU ranges from 0 to 1023.

$$DT - RDMLU = [H - DTRDMLU1; H - DTRDMLU2; H - DTRDMLU3; H - DTRDMLU4]$$

Finally, the feature vectors of CT-RDMLU and DT-RDMLU are concatenated to derive Cross & Diagonal-Rule based Directional Motif -Local unit (CD-RDMLU).

$$CD-RDMLU = (CT-RDMLU, DT-RDMLU) \tag{9}$$

The Feature vector of CD-RDMLU ranges from 0 to 2046. The histograms of these feature vector will derive the final feature vector. The entire process of generating CD-RDMLU is given in the following algorithm and the framework is shown in fig 13.

Algorithm begin

Input: image: output: Retrieval results

1. Convert the image into grayscale image
2. Divide the image into 3 x 3 grids (overlapped manner)
 - 2a. Partition the image window into cross matrix and diagonal matrix.
3. Derive the four CTDM's (CTDM1.... CTDM4) on cross matrix
4. Derive the four DTDM's (DTDM1.... DTDM4) on diagonal matrix.
5. Derive CT-DRM indexes (Directional Rule based motif indexes)

for each of CTDM1.... CTDM4 and DTDM1.... DTDM4. This Process creates 8 different triangular Directional Rule based motif images (CTRDM1 to CTRDM4 and DTRDM1 to DTRDM4 images).

6. Transform the CTRDM1 to CTRDM4 images into CT-RDMLU1 to CT-RDMLU4 and Construct histogram for each of CT-RDMLU and concatenate them to derive CT-RDMLU.
7. Transform the DTRDM1 to DTRDM4 images into DT-RDMLU1 to DT-RDMLU4 images and Construct histogram for each of DT-RDMLU and concatenate them to derive DT-RDMLU.
8. Construct the feature vector of CD-RDMLU by concatenating histograms of CT-RDMLU and DT-RDMLU.
9. Compare the query image features with features in the database image.
10. (8) Retrieve the images based on the best matches

End of the algorithm

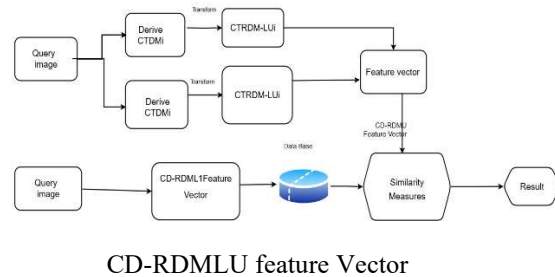


Fig 13. Proposed Cbir System Frame Work

Database description

The Corel-1K and Corel-10K image databases were sourced from the Corel photo gallery and contain natural images. The Corel-10K database features a diverse collection of images, including categories such as bonsai, dogs, icebergs, elephants, aviation, autumn, tigers, steam engines, and waterfalls. It contains 10,800 images across 80 different categories, with a varying number of images per category, but each category includes at least 100 images. The images in Corel-10K are sized at 120x86 pixels. The Corel-1K database, on the other hand, contains 1,000 images divided into 10 categories, with 100 images per category. Both the Corel-1K and Corel-10K databases are well-suited for image

retrieval research due to their large, varied, and homogeneous image sets within each category. The MIT-VisTex database, consisting of high-quality texture images, was created as an alternative to the older and now partially unavailable Brodatz texture database. The MIT-VisTex images are representative of real-world texture conditions, offering a modern resource for texture-based image analysis. The CMU Multi-PIE database contains facial images and is one of the largest facial image datasets, featuring 337 subjects and a total of 750,000 images. It covers four sessions with a 15-month gap between them, offering 15 viewpoints and 19 illumination conditions, totaling more than 300 GB of image data. For this research, 15 categories of facial images were selected, with each category containing 150 images. Additionally, this study utilized the Holidays dataset, which consists of 500 image groups, primarily comprising personal holiday photographs. The image samples of these databases are shown from **Fig. 14 to Fig. 18**.

3. RESULTS AND DISCUSSION

This paper used Euclidean distance measure to compute the similarity measure between the query image and database images. The average precision rate (APR) and average retrieval rate (ARR) are used as metrics to evaluate the performance of the proposed method, on the 5-benchmark databases as discussed above. These databases are considered to the following reasons: (i) images of different categories (ii) captured with different backgrounds (iii) captured under varying viewing angles, lightening conditions, etc... The proposed CD-RDMLU feature vector is computed for all databases images. When the query image is presented, the proposed CD-RDMLU feature vector is computed and the distance measure is used to pick up the relative images. The APR and ARR for the top 10 images retrieved by the proposed CD-RDMLU are summarized in Table 1.

Table 1: APR and ARR for the top 10 matches by CD-RDMLU

Parameter	Co rel - 1K	Co rel - 10K	MIT Vis tex	Bro dtaz	C M U P I E	Ave rage
APR	92.49	57.21	93.15	92.19	95.65	86.13

ARR	49.2	38.29	94.56	89.25	96.24	73.50
-----	------	-------	-------	-------	-------	-------

The average performance of all the five databases are compared with the existing methods by using APR and ARR on each databases and plotted in the following graphs. The retrieved top 20 images from each database by the CD-RDMLU for the given query image is shown from **Fig X to Y**. This paper noted the following significances of the proposed method based on the above results.

1. The CD-RDMLU achieved high retrieval rate for core-1K when composed to coral-10K, due to few number of classes, few number of backgrounds that were present in core-1K when compared to coral 10K.
2. The proposed method exhibited high retrieval rate for the CMG-PIE and MIT-VISTEX data base images when compared to the other databases.
3. The basic reasons for the proposed methods domination in terms of APR and ARR when compared to the other existing methods on all databases are due to (i) the estimation of motif features on Cross and diagonal matrices (ii) the derivation of Triangular directional motifs (iii) the novelty of the proposed RDM in addressing the ambiguity issues and derivation of unique motif indexes (iv) the transformation of input image into eight CD-RDMLU images, and derivation of a powerful feature vector that captures the structural, statistical, edge, texture, pattern and, directional features of the image.

Main contribution of the proposed method.

1. Extraction of Triangular directional motifs on a 3*3 grid by partitioning into cross and diagonal matrices.
2. Derivation of Rule based directional motif (RDM) to overcome the ambiguities and to define a unique motif when two or all three pixels exhibits the same intensity levels.
3. Transformation of CT-RDM and DT-RDM into CTRDMLU and DTRDMLU images.
4. Concatenation of CTRDMLU and DTRDMLU features and deriving powerful CD-RDMLU features, that holds the edge, structural, texture, directional, statistical, and pattern based features of the image.



Fig. 14: The Illustration Of Corel-1K Images



Fig. 15: A Few Example Images Of Corel-10K



Fig. 16: A Few Instance From MIT-Vistex

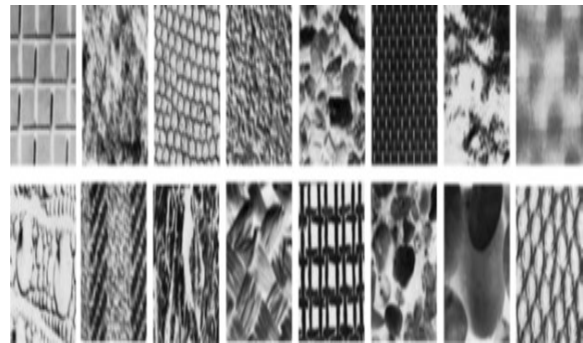


Fig. 17: A few Brodatz textures



Fig. 18: A Few CMU-PIE Facial Images

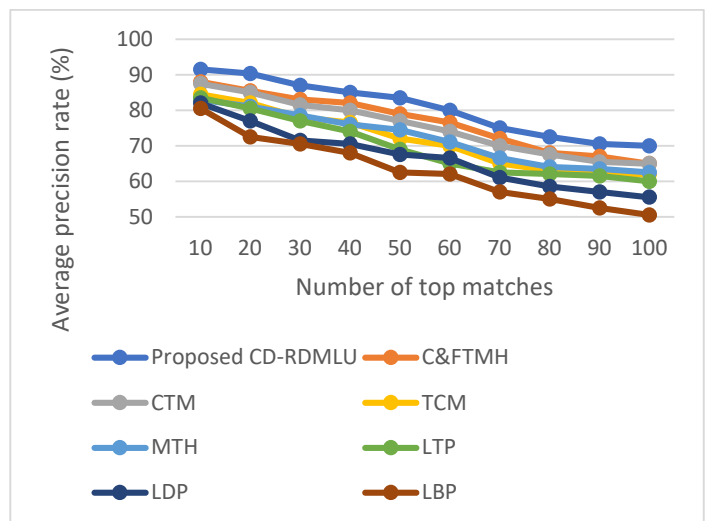


Fig. 19. Corel 1 K On APR: Existing Descriptors Vs CD-RDMLU Descriptor

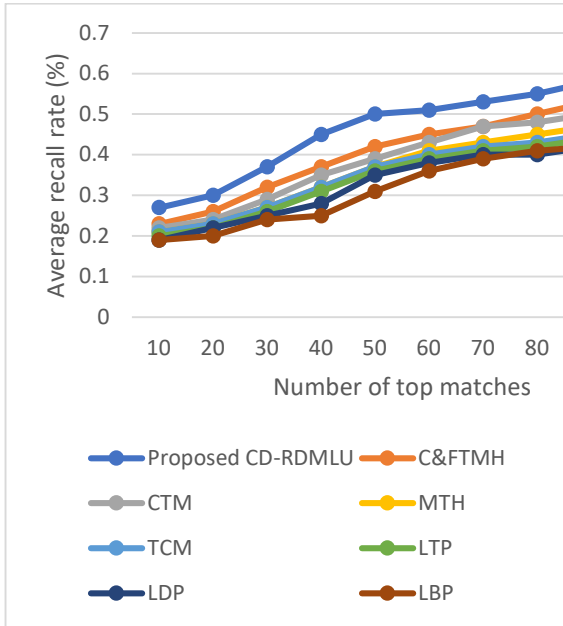


Fig.20. Corel 1 K On ARR: Existing Descriptors Vs CD-RDMLU Descriptor

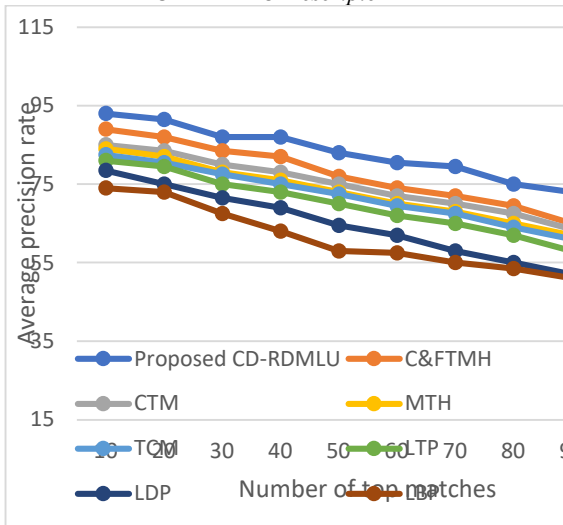


Fig. 21. APR On Corel 10K: Existing Methods Vs Proposed CD-RDMLU

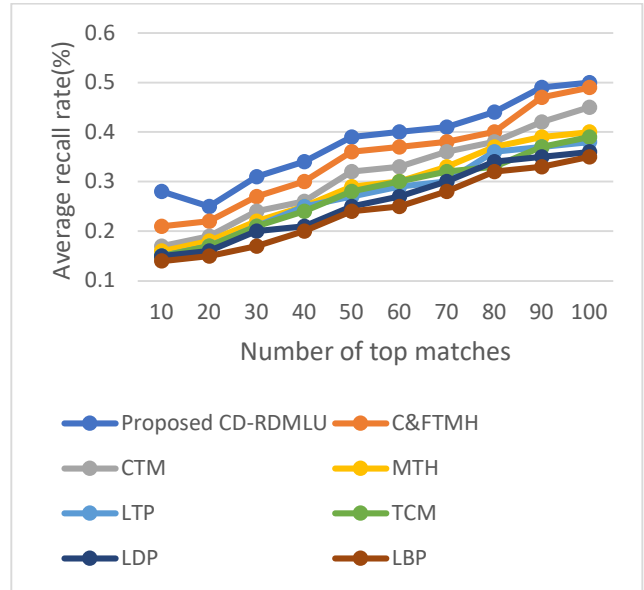


Fig. 22. ARR On Corel 10K: Existing Methods Vs Proposed CD-RDMLU

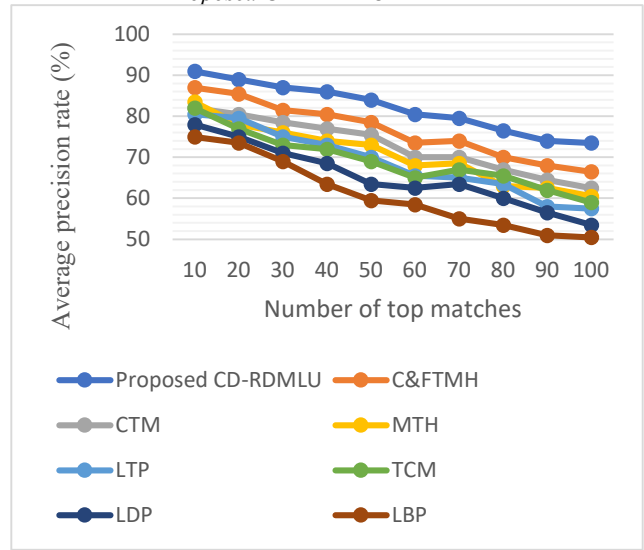


Fig. 23. MIT-Vistex: Using APR : Proposed Descriptor Vs Prevailing Methods

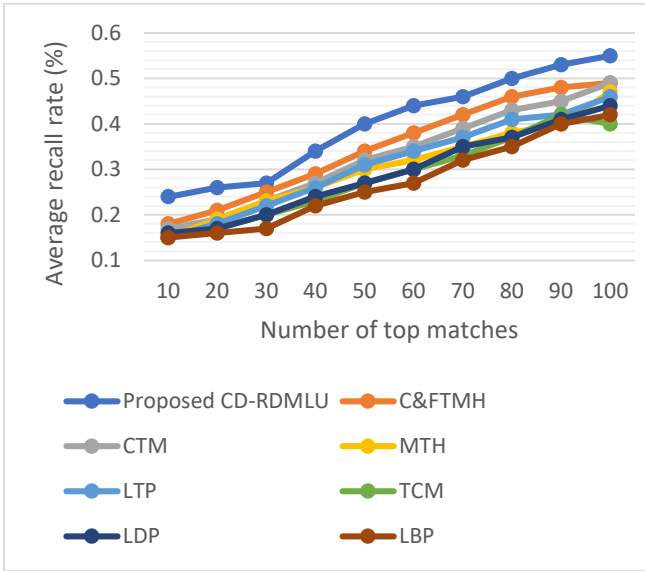


Fig. 24. ARR : MIT-Vistex Database” Proposed vs existing methods

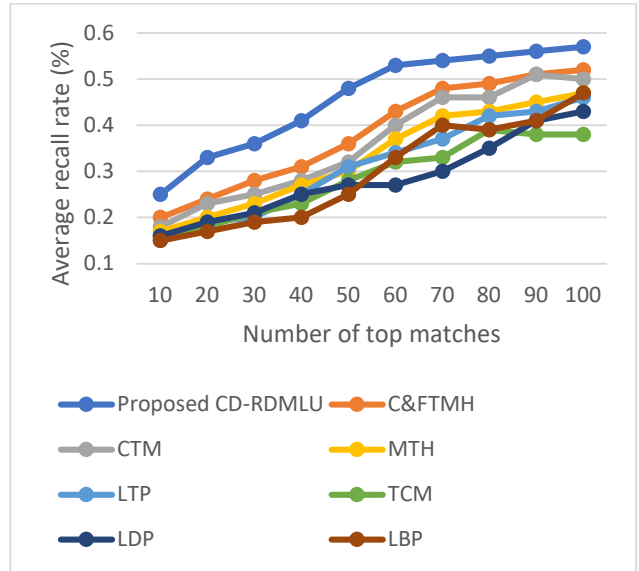


Fig. 26. ARR: Brodatz Database : Proposed Versus Existing Approaches

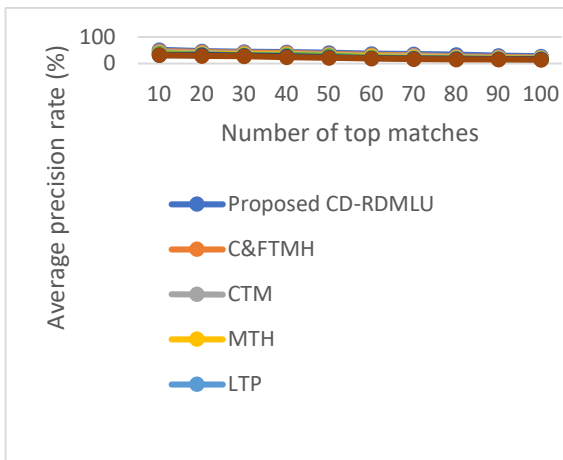


Fig. 25. The CD-RDMLU Versus Existing Methods On Brodatz Database Using APR

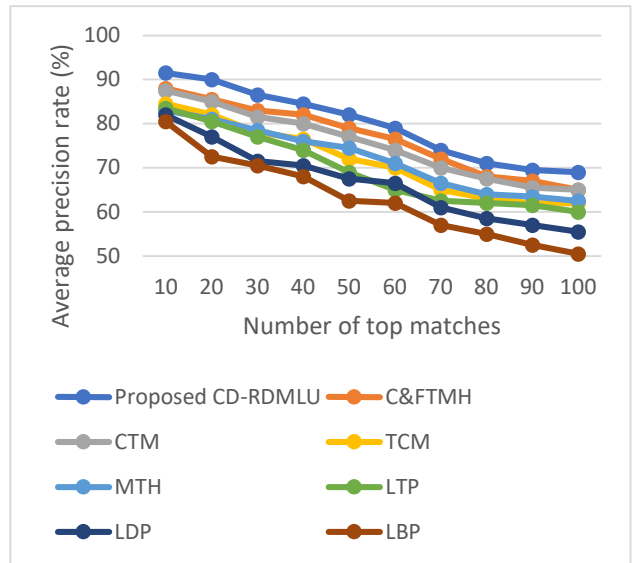


Fig. 21. Proposed CD-RDMLU Vs Existing Descriptors: CMU-PIE Database : APR

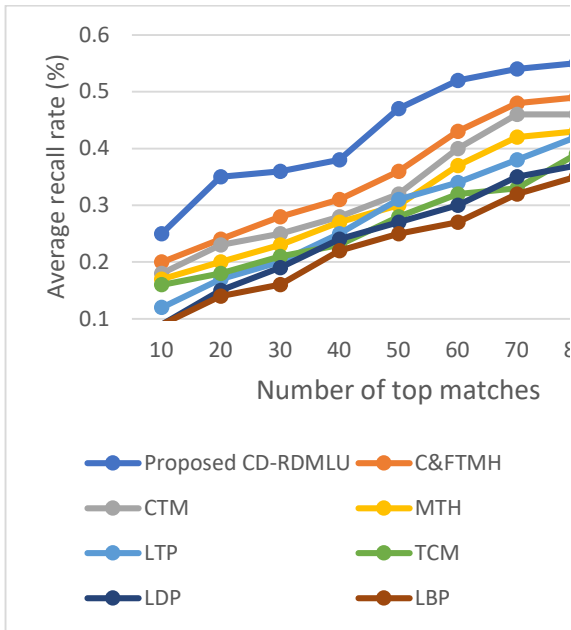


Fig. 22. ARR: CD-RDMLU Versus Existing Methods: Over CMU-PIE

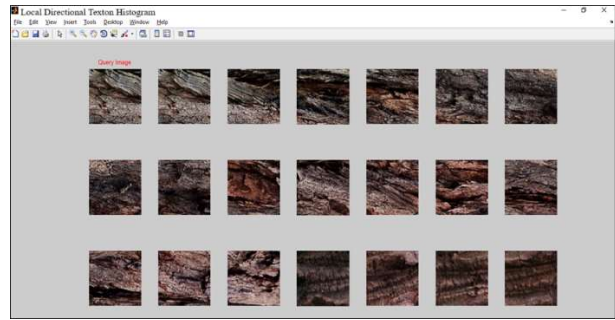


Fig. 25. The Top 20 Retrievals From CD-RDMLU Over MIT-Vistex

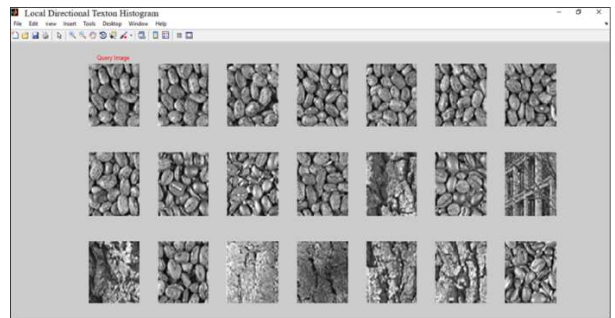


Fig. 26. Brodatz Database: The Top 20 Retrievals

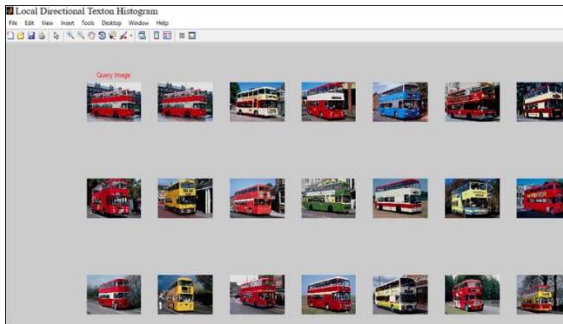


Fig. 23. Corel-1k : The Top 20 Retrievals By CD-RDMLU

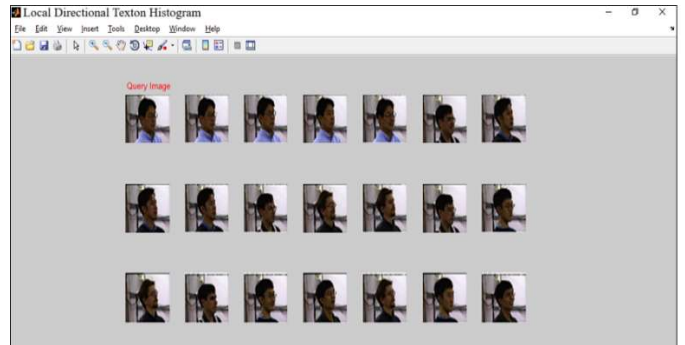


Fig. 27 Top 20 Retrievals From CMU-PIE Database



Fig. 24. The Top 20 Retrievals: Corel-10k Database

4. CONCLUSION

The proposed CD-RDMLU achieved high retrieval rate in terms of APR and ARR when compared to the existing methods. The division of 3*3 windows into two micro windows namely cross and diagonal grids, and deriving the micro of micro level local features by subdividing each cross and diagonal grids into four triangular micro grids and deriving motif indexes on this. The triangular motif features derive structural, edge, directions and features at the micro of micro level. The derived RDM overcomes the ambiguity thus improved overall performance. Further the transformation of each of motif triangular indexes into a 3*3 window and the

derived local features on this extracted statistical and texture features in addition to the above mentioned features. The combination of eight local features sets derived from the cross and diagonal triangular RDM's extracted micro of micro and local features and the combinations of these features derived a potential source for high retrieval rate.

REFERENCES

- [1] Agarwal M, Singhal A, Lall B (2019) Multi-channel local ternary pattern for content-based image retrieval. Springer, Pattern Analysis and Applications, pp 1–12
- [2] Bian W, Tao D (2010) Biased Discriminant Euclidean Embedding for content-based image retrieval. *IEEE Trans Image Process* 19(19):545–555
- [3] Dubey SR, Singh SK, Singh RK (2016) Multichannel decoded local binary patterns for content-based image retrieval. *IEEE Trans Image Process* 25(9):4018–4032
- [4] Hiremath PS (2007) Content Based Image Retrieval using color, Texture and shape features. In: 15th International Conference on Advanced Computing and Communications. © 2007 IEEE computer society
- [5] Husain S, Bober M (2017) Improving large-scale image retrieval through robust aggregation of local descriptors. *IEEE Transactions on Pattern Analysis and Machine Intelligence*
- [6] Lai C-C, Chen Y-C (2011) A User-Oriented Image Retrieval System Based on Interactive Genetic Algorithm. *IEEE Transactions on Instrumentation and Measurement* 60(10):3318–3325
- [7] Srivastava P, Khare A (2018) Utilizing multiscale local binary pattern for content-based image retrieval. Springer, *Multimed Tools Appl*, 77(10):1237
- [8] Subash Kumar TG, Nagarajan V (2018) Local curve pattern for content-based image retrieval. In: Pattern Analysis and Applications. Springer, pp 1–10
- [9] Yang J, Jiang B, Li B, Tian K, Lv Z (2017) A fast image retrieval method designed for network big data. *IEEE Transactions on Industrial Informatics* 13(5):2350–2359
- [10] Zhang J, Yoo C-W, Ha S-W (2007) ROI Based Natural Image Retrieval using Color and Texture Feature. In: 4th International Conference on Fuzzy system and Knowledge Discovery
- [11] Ahmed KT, Ummesafi S, Iqbal A (2019) Content based image retrieval using image features information fusion. *Inf Fusion* 51:76–99
- [12] Lu H, Zhang M, Xu X, Li Y, Shen HT (2020) Deep fuzzy hashing network for efficient image retrieval. *IEEE transactions on fuzzy systems*
- [13] Sathiamoorthy S, Natarajan M (2020) An efficient content based image retrieval using enhanced multi- trend structure descriptor. *SN Applied Sciences* 2(2):1–20
- [14] Tsochatzidis L, Zagoris K, Arikidis N, Karahaliou A, Costaridou L, Pratikakis I (2017) Computer-aided diagnosis of mammographic masses based on a supervised content-based image retrieval approach. *Pattern Recogn* 71:106–117
- [15] Yan C, Li L, Zhang C, Liu B, Zhang Y, Dai Q (2019) Cross-modality bridging and knowledge transferring for image understanding. *IEEE Trans Multimed* 21(10):2675–2685
- [16] Afifi AJ, Ashour WM (2012) "Content-Based Image Retrieval Using Invariant Color and Texture Features," 2012 International conference on digital image computing techniques and applications (DICTA), Fremantle, WA, pp. 1–6, <https://doi.org/10.1109/DICTA.2012.6411665>.
- [17] Belloulata K, Belallouche L, Belalia A, Kpalma K (2014) "Region based image retrieval using Shape- Adaptive DCT," 2014 IEEE China Summit & International Conference on Signal and Information Processing (ChinaSIP), Xi'an, pp. 470–474, <https://doi.org/10.1109/ChinaSIP.2014.6889287>.
- [18] Bhagat AP, Atique M (2012) "Design and development of systems for image segmentation and content based image retrieval," 2012 2nd National Conference on computational intelligence and signal processing (CISP), Guwahati, Assam, pp. 109–113, <https://doi.org/10.1109/NCCISP.2012.6189688>.
- [19] Chen J et al (2010) WLD: a robust local image descriptor. *IEEE Trans Pattern Anal Mach Intell* 32(9): 1705–1720. <https://doi.org/10.1109/TPAMI.2009.155>
- [20] Choudhary R, Raina N, Chaudhary N, Chauhan R, Goudar RH (2014) "An

- integrated approach to content based image retrieval," 2014 international conference on advances in computing, Communications and Informatics (ICACCI), New Delhi, pp. 2404-2410, <https://doi.org/10.1109/ICACCI.2014.6968394>.
- [21] Dubey SR (2019) Face retrieval using frequency decoded local descriptor. *Multimed Tools Appl* 78:16411–16431. <https://doi.org/10.1007/s11042-018-7028-8>
- [22] Rasli RM, Muda TZZ, Yusof Y, Bakar JA (2012) "Comparative Analysis of Content Based Image Retrieval Techniques Using Color Histogram: A Case Study of GLCM and K-Means Clustering," 2012 Third international conference on intelligent systems modelling and simulation, Kota Kinabalu, pp. 283–286, <https://doi.org/10.1109/ISMS.2012.111>.
- [23] Redi M, Merialdo B (2011) "Saliency-aware color moments features for image categorization and retrieval," 2011 9th International Workshop on Content-Based Multimedia Indexing (CBMI), Madrid, pp. 199–204, <https://doi.org/10.1109/CBMI.2011.5972545>.
- [24] Selvarajah S, Kodithuwakku SR (2011) "Combined feature descriptor for Content based Image Retrieval," 2011, 6th International Conference on Industrial and Information Systems, Kandy, pp. 164–168, <https://doi.org/10.1109/ICIINFS.2011.6038060>.
- [25] Singh N, Singh K, Sinha AK (2012) A novel approach for content based image retrieval. *Procedia Technol* 4:245–250
- [26] Singh C, Walia E, Kaur KP (2018) Color texture description with novel local binary patterns for effective image retrieval. *Pattern Recog* 76:50–68
- [27] Varish N, Pal AK (2015) "Content based image retrieval using statistical features of color histogram," 2015 3rd international conference on signal processing, Communication and Networking (ICSCN), Chennai, pp. 1-6, <https://doi.org/10.1109/ICSCN.2015.7219922>.
- [28] Vatamanu OA, Franduş M, Lungeanu D, Mihalaş GI (2015) Content based image retrieval using local binary pattern operator and data mining techniques. *Stud Health Technol Inform* 210:75–79
- [29] Wenfei D, Shuchun Y, Songyu L, Zhiqiang Z, Wenbo G (2014) "Image retrieval based on multi-feature fusion," 2014 fourth international conference on instrumentation and measurement. *Computer, Communication and Control*, Harbin, pp 240–243. <https://doi.org/10.1109/IMCCC.2014.57>
- [30] Yasmin M, Sharif M, Irum I, Mohsin S (2014) An efficient content based image retrieval using EI classification and color features. *J Appl Res Technol* 12(5):877–885